# Flow and heat transfer of a nanofluid over a hyperbolically stretching sheet*

A. Ahmad[a)†], S. Asghar[a)b)], and A. Alsaedi[b)]

[a)] *COMSATS Institute of Information Technology, Islamabad, Pakistan*

[b)] *Distinguished Adjunct Professor, Department of Mathematics, King Abdul Aziz University, Jeddah, Saudi Arabia*

(Received 13 September 2013; revised manuscript received 1 January 2014; published online 22 May 2014)

This article explores the boundary layer flow and heat transfer of a viscous nanofluid bounded by a hyperbolically stretching sheet. Effects of Brownian and thermophoretic diffusions on heat transfer and concentration of nanoparticles are given due attention. The resulting nonlinear problems are computed for analytic and numerical solutions. The effects of Brownian motion and thermophoretic property are found to increase the temperature of the medium and reduce the heat transfer rate. The thermophoretic property thus enriches the concentration while the Brownian motion reduces the concentration of the nanoparticles in the fluid. Opposite effects of these properties are observed on the Sherwood number.

**Keywords:** hyperbolically stretching sheet, nanofluid, boundary layer flow heat transfer

**PACS:** 44.20.+b, 44.05.+e, 47.15.−x **DOI:** 10.1088/1674-1056/23/7/074401

## 1. Introduction

Nanofluids are engineered colloids made of the fluids and nanoparticles (1 nm–100 nm), with high thermal conductivity and heat transfer. Nanoparticles, as compared to milli and micro sized particles, are close in size to the molecules of the base fluid with very stable suspension with little gravitational settling over a long period of time. Alumina oxide, silica oxide, titania oxide copper oxide and some metals (like copper and gold) are some commonly used nanoparticles. The volumetric fraction of the nanoparticles is usually below 5%.

In 1993, Masuda *et al.*[1] reported the thermal conductivity enhancement in liquid dispersions of nanofluid. Several attempts are made to develop the convective transport model for nanofluids. A homogenous flow model was proposed by Choi[2] in which he directly extends the equations of a pure fluid to a nanofluid. Another model is the dispersion model, which is based on the observation that the convective heat transfer enhancement in nanofluids comes from the high thermal conductivity and dispersion of nanofluids.

The homogenous flow model is in conflict with the experimental observation.[3] Buongiorno,[3] rejecting the dispersion model, showed that the heat transfer for nanoparticles dispersion is completely negligible in nanofluids. He proposed an alternative model that eliminates the short comings of the two above mentioned models. According to this model, the naoparticle absolute velocity can be viewed as the sum of the base fluid velocity and the relative (slip) velocity and considered seven slip mechanisms: inertia, Brownian diffusion, thermophoresis, diffusiophoresis, the Magnus effect, fluid drainage, and gravity settling. After examining each of these in turn, he concluded that in the absence of turbulent effects, it is the Brownian and the thermophoresis diffusions that will be important. Some recent analysis on the heat transfer mechanism in nanofluids can be found in Refs. [4]–[7] and the references therein.

The study of flow and heat transfer over a continuous stretching sheet with a given temperature distribution has received much attention due to its applications in different fields of engineering and industry. The stretching and heating/cooling of the plate have a definite impact on the quality of the finished product. Examples of such processes are extrusion of polymers, aerodynamic extrusion of plastic sheets and the condensation process of metallic plate. Modeling the real processes is thus undertaken with the help of different stretching velocities and surface temperature distributions. These are linear,[8] polynomial,[9–11] exponential[12] and hyperbolic[13] stretching velocities.

For instance, Bachok *et al.*[13] studied the flow of nanofluid over a moving surface. Khan and Pop[14] numerically investigated the problem of laminar flow of nanofluid due to stretching of the surface. They used the model of the nanofluid, which integrates the effects of thermophoresis and Brownian motion and obtained the similarity solution. Rana and Bhargava[15] investigated the nanofluid flow, which results from the non-linear stretching sheet. Nadeem and Lee[16] presented the flow and heat transfer of nanofluid over an exponentially stretching sheet.

Considering the significance of nanoscience in the present era, it is desirable to look for the possibility of other stretching velocities and the surface temperature distributions for nanofluids. The aim of this paper is to present the study of

*Project supported by the CIIT Research Grant Program (CRGP) of COMSATS Institute of Information Technology, Islamabad, Pakistan (Grant No. 16-69/CRGP/CIIT/IBD/10/711).

†Corresponding author. E-mail: adeelahmed@comsats.edu.pk

© 2014 Chinese Physical Society and IOP Publishing Ltd 

the flow and heat transfer of a nanofluid over a hyperbolically stretching sheet.[13]

## 2. Development of problem

We consider the two-dimensional flow of viscous nanofluid induced by a stretching surface at $Y=0$. Here, the $X$ axis is chosen along the surface whereas the $Y$ axis is taken to be normal to the surface. The flow is chosen for $Y>0$. At the sheet, the temperature $T$ and the nanoparticle fraction $\phi$ have values $T_{\rm w}$ and $\phi_{\rm w}$, respectively. The ambient values $T_\infty$ and $\phi_\infty$ of $T$ and $\phi$ are attained when $Y$ tends to infinity. The boundary layer problem is governed by the following expressions:

$$\frac{\partial U}{\partial X}+\frac{\partial V}{\partial Y}=0, \tag{1}$$

$$\rho_{\rm f}\Big(U\frac{\partial U}{\partial X}+V\frac{\partial U}{\partial Y}\Big)=\mu\frac{\partial^2 U}{\partial Y^2}, \tag{2}$$

$$U\frac{\partial T}{\partial X}+V\frac{\partial T}{\partial Y}=\alpha\frac{\partial^2 T}{\partial Y^2}+\tau\Big[D_{\rm B}\frac{\partial T}{\partial Y}\frac{\partial \phi}{\partial Y}+\frac{D_{\rm T}}{T_\infty}\Big(\frac{\partial T}{\partial Y}\Big)^2\Big], \tag{3}$$

$$U\frac{\partial \phi}{\partial X}+V\frac{\partial \phi}{\partial Y}=D_{\rm B}\frac{\partial^2 \phi}{\partial Y^2}+\frac{D_{\rm T}}{T_\infty}\frac{\partial^2 T}{\partial Y^2}. \tag{4}$$

We notice that in Eqs. (1)–(4), $(U,V)$ are the velocity components in the $(X,Y)$ directions respectively. The $\rho_{\rm f}$ is the base fluid density and $\mu$, $\alpha$, and $\beta$ are the viscosity, thermal conductivity and volumetric volume expansion coefficient of the nanofluid, while $\rho_{\rm p}$ is the density of the particles. Further $D_{\rm B}$ and $D_{\rm T}$ are the Brownian and thermophoretic diffusion coefficients and $\alpha$ and $\tau$ are defined as

$$\alpha=\frac{k}{(\rho c)_{\rm f}},\quad \tau=\frac{(\rho c)_{\rm p}}{(\rho c)_{\rm f}}.$$

The subjected boundary conditions can be written as

$$\begin{aligned}&U(X,Y)=U_{\rm w}(x),\ \ V(X,Y)=0,\ \ T(X,Y)=T_{\rm w}(X),\\&\phi(X,Y)=\phi_{\rm w}(X)\ \ \text{at}\ \ Y=0,\\&U(X,Y)\to 0,\ \ T(X,Y)=T_\infty,\ \ \phi(X,Y)=\phi_\infty\ \ \text{as}\ \ Y\to\infty,\end{aligned} \tag{5}$$

where $T_{\rm w}(X)=T_\infty+A_1\,(U_{\rm w}(X))^2$, $\phi_{\rm w}(X)=\phi_\infty+A_2U_{\rm w}(X)$, and $u_{\rm o}, A_1, A_2$ are dimensional constants. Using the transformation

$$\Psi=\nu Re_x^{1/2}f(\eta,x),\ \ \theta(\eta,x)=\frac{T-T_\infty}{T_{\rm w}-T_\infty},\ \ s(\eta,x)=\frac{\phi-\phi_\infty}{\phi_{\rm w}-\phi_\infty}, \tag{6}$$

in Eqs. (1)–(5) yields

$$f'''+\frac{1}{2}\Big(1+\frac{x}{U_{\rm w}}\frac{{\rm d}U_{\rm w}}{{\rm d}x}\Big)ff''-\frac{x}{U_{\rm w}}\frac{{\rm d}U_{\rm w}}{{\rm d}x}f'^2=x\Big(f'\frac{\partial f'}{\partial x}-f''\frac{\partial f}{\partial x}\Big), \tag{7}$$

$$\theta''-Pr\frac{x}{\Delta T}\frac{{\rm d}\Delta T}{{\rm d}x}f'\theta+\frac{Pr}{2}\Big(1+\frac{x}{U_{\rm w}}\frac{{\rm d}U_{\rm w}}{{\rm d}x}\Big)f\theta'+N_{\rm bx}\theta's'+N_{\rm tx}(\theta')^2=Prx\Big(f'\frac{\partial\theta}{\partial x}-\theta'\frac{\partial f}{\partial x}\Big), \tag{8}$$

$$s''-Le\frac{x}{\Delta\phi}\frac{{\rm d}\Delta\phi}{{\rm d}x}f's+\frac{Le}{2}\Big(1+\frac{x}{U_{\rm w}}\frac{{\rm d}U_{\rm w}}{{\rm d}x}\Big)fs'+\frac{N_{\rm tx}}{N_{\rm bx}}\theta''=Lex\Big(f'\frac{\partial s}{\partial x}-s'\frac{\partial f}{\partial x}\Big), \tag{9}$$

$$f'=1,\ \ f=0,\ \ \theta=1,\ \ s=1\ \ \text{at}\ \ \eta=0,\quad f'\to 0,\ \ \theta\to 0,\ \ s\to 0\ \ \text{as}\ \ \eta\to\infty, \tag{10}$$

in which

$$\eta=\frac{Y}{X}Re_x^{1/2},\ \ x=\frac{X}{L},\ \ Re_x=\frac{U_{\rm w}(X)X}{\nu},$$

is the local Reynold number, $\nu$ is the kinematic viscosity of the nanofluid, $N_{\rm bx}$ is the local Brownian motion parameter, $N_{\rm tx}$ is the local thermophoresis parameter, $Pr$ and $Le$ are the Prandtl and Lewis numbers with the following expressions:

$$N_{\rm b}=\frac{\tau D_{\rm B}\Delta\phi}{\alpha},\ \ N_{\rm t}=\frac{\tau D_{\rm T}\Delta T}{\alpha T_\infty},\ \ Le=\frac{\nu}{D_{\rm B}},\ \ Pr=\frac{\nu}{\alpha}.$$

Equations (7)–(10) after taking the hyperbolic stretching velocity $U_{\rm w}(x)=u_0\sinh(x)$ give

$$f'''+\frac{1}{2}\left[1+x\coth(x)\right]ff''-x\coth(x)\,f'^2=x\Big(f'\frac{\partial f'}{\partial x}-f''\frac{\partial f}{\partial x}\Big), \tag{11}$$

$$\theta''+\frac{Pr}{2}\left[1+x\coth(x)\right]f\theta'-2Prx\coth(x)\,f'\theta+N_{\rm b}\sinh(x)\theta's'+N_{\rm t}(\sinh(x))^2(\theta')^2=x\Big(f'\frac{\partial\theta}{\partial x}-\theta'\frac{\partial f}{\partial x}\Big), \tag{12}$$

$$s''+\frac{Le}{2}\left[1+x\coth(x)\right]fs'-Lex\coth(x)\,f's+\frac{N_{\rm t}}{N_{\rm b}}\sinh(x)\theta''=Lex\Big(f'\frac{\partial s}{\partial x}-s'\frac{\partial f}{\partial x}\Big), \tag{13}$$

where

$$N_{\rm b}=\frac{\tau D_{\rm B}A_2u_0}{\alpha},\quad N_{\rm t}=\frac{\tau D_{\rm T}A_2u_0^2}{\alpha T_\infty}$$

are the Brownian motion and thermophoresis parameters respectively.

## 3. Solution methodologies

For the problem under consideration, the analytical solution is developed by a series expansion method for small $x$ and the LNS method is implemented for the numerical solution.

### 3.1. Series solution for small $x$

We write $f(\eta,x)$, $\theta(\eta,x)$, and $s(\eta,x)$ in power of $x$ as follows:

$$\begin{aligned}f(\eta,x)&=f_0(\eta)+xf_1(\eta)+x^2f_2(\eta)+\ldots,\\\theta(\eta,x)&=\theta_0(\eta)+x\theta_1(\eta)+x^2\theta_2(\eta)+\ldots,\\s(\eta,x)&=s_0(\eta)+xs_1(\eta)+x^2s_2(\eta)+\ldots\end{aligned} \tag{14}$$

Substituting Eq. (14) into Eqs. (10)–(13) and then equating the terms of $O(1)$, we have the following leading order system:

$$f_0'''+f_0f_0''-f_0'^2=0, \tag{15}$$

$$\theta_0''+Prf_0\theta_0'-2Prf_0'\theta_0=0, \tag{16}$$

$$s_0'' + Le f_0 s_0' - 2Le f_0' s_0 = 0, \tag{17}$$

$$f_0' = 1,\ \ f_0 = 0,\ \ \theta_0 = 1,\ \ s_0 = 1 \ \text{ at } \ \eta = 0,$$
$$f_0' \to 0,\ \ \theta_0 \to 0,\ \ s_0 \to 0,\ \ \text{as } \ \eta \to \infty. \tag{18}$$

Solving the above problem, we have

$$f_0(\eta) = 1 - \mathrm{e}^{-\eta}, \tag{19}$$

$$\theta_0(\eta) = \mathrm{e}^{-Pr\eta}\frac{\mathrm{Ku}(Pr-2, Pr+1, -Pr\mathrm{e}^{-\eta})}{\mathrm{Ku}(Pr-2, Pr+1, -Pr)}, \tag{20}$$

$$s_0(\eta) = \mathrm{e}^{-Le\eta}\frac{\mathrm{Ku}(Le-1, Le+1, -Le\mathrm{e}^{-\eta})}{\mathrm{Ku}(Le-1, Le+1, -Le)}. \tag{21}$$

The solutions (19)–(21) represents the flow of a traditional viscous fluid over a linearly stretching surface with heat and mass transfer. The system of $O(x)$ can be written as

$$f_1''' + f_0 f_1'' - 3f_0' f_1' + 2f_0'' f_1 = 0, \tag{22}$$

$$\theta_1'' + Pr f_0 \theta_1' - 3Pr f_0' \theta_1 = -N_\mathrm{b}\theta_0' s_0', \tag{23}$$

$$s_1'' + Le f_0 s_1' - 2Le f_0' s_1 = -\frac{N_\mathrm{t}}{N_\mathrm{b}}\theta_0''. \tag{24}$$

$$f_1'(\eta) = 0,\ \ f_1(\eta) = 0,\ \ \theta_1(\eta) = 0,\ \ s_1(\eta) = 0 \ \text{ at } \ \eta = 0,$$
$$f_1'(\eta) \to 0,\ \ \theta_1(\eta) \to 0,\ \ s_1(\eta) \to 0 \ \text{ as } \ \eta \to \infty. \tag{25}$$

To find the solution of the above problem, we use $\xi = \mathrm{e}^{-\eta}$ in Eqs. (22)–(25). Whereas the series solution of system (22)–(25) can be obtained for different values of the parameters involved, it suffices to present the solution for $Pr = 1$, $Le = 2$, $N_\mathrm{t} = 0.1$, and $N_\mathrm{b} = 0.1$. Thus the series solution, written in the variable $\eta$, is given by

$$f_1(\eta) = 0, \tag{26}$$

$$\theta_1(\eta) = 0.0545(1 - \mathrm{e}^{-\eta}) - 0.125(1 - \mathrm{e}^{-\eta})^2 - 0.0705(1 - \mathrm{e}^{-\eta})^3, \tag{27}$$

$$s_1(\eta) = 1.2307(1 - \mathrm{e}^{-\eta}) - 1.3846(1 - \mathrm{e}^{-\eta})^2 - 0.1538(1 - \mathrm{e}^{-\eta})^3. \tag{28}$$

Employing the procedure of the previous chapter, the problem statement and solution for the $O(x^2)$ system are

$$f_2''' + f_0 f_2'' - 4f_0' f_2' + 3f_0'' f_2 = -\left(2f_1'' f_1 - 2f_1'^2 + \frac{1}{6}f_0'' f_0 - \frac{1}{3}f_0'^2\right), \tag{29}$$

$$\theta_2'' + Pr f_0 \theta_2' - 4Pr f_0' \theta_2 = -\left(3Pr\theta_0' f_2 - 2Pr\theta_0 f_2' + \frac{Pr}{6}\theta_0' f_0 - \frac{2}{3}Pr f_0'\theta_0 + N_\mathrm{t}\theta_0'^2 + N_\mathrm{b}\theta_0' s_1' + N_\mathrm{b}\theta_1' s_0'\right), \tag{30}$$

$$s_2'' + Le f_0 s_2' - 3Le f_0' s_2 = -\left(3Les_0' f_2 - Les_0 f_2' + \frac{Le}{6}s_0' f_0 - \frac{Le}{3}f_0' s_0 + \frac{N_\mathrm{t}}{N_\mathrm{b}}\theta_1''\right), \tag{31}$$

$$f_2'(\eta) = 0,\ \ f_2(\eta) = 0,\ \ \theta_2(\eta) = 0,\ \ s_2(\eta) = 0 \ \text{ at } \ \eta = 0,$$
$$f_2'(\eta) \to 0,\ \ \theta_2(\eta) \to 0,\ \ s_2(\eta) \to 0 \ \text{ as } \ \eta \to \infty, \tag{32}$$

and

$$f_2(\eta) = -0.02777(1 - \mathrm{e}^{-\eta})^2 - 0.02777(1 - \mathrm{e}^{-\eta})^3, \tag{33}$$

$$\theta_2(\eta) = -0.2248(1 - \mathrm{e}^{-\eta}) + 0.4815(1 - \mathrm{e}^{-\eta})^2 + 0.2567(1 - \mathrm{e}^{-\eta})^3, \tag{34}$$

$$s_2(\eta) = -0.221(1 - \mathrm{e}^{-\eta}) + 0.375(1 - \mathrm{e}^{-\eta})^2 + 0.1542(1 - \mathrm{e}^{-\eta})^3. \tag{35}$$

### 3.2. Numerical solution (LNS method)

Here we introduce two new functions as

$$g(\eta, x) = \frac{\partial f}{\partial x},\ \ \varphi(\eta, x) = \frac{\partial \theta}{\partial x},\ \ h(\eta, x) = \frac{\partial s}{\partial x}, \tag{36}$$

Omitting the terms

$$x\left(f'\frac{\partial f'}{\partial x} - f''\frac{\partial f}{\partial x}\right),\ \ x\left(f'\frac{\partial \theta}{\partial x} - \theta'\frac{\partial f}{\partial x}\right),\ \ x\left(f'\frac{\partial s}{\partial x} - s'\frac{\partial f}{\partial x}\right)$$

in Eqs. (11)–(13) respectively one has

$$f''' + \frac{1}{2}[1 + x\coth(x)]ff'' - x\coth(x)f'^2 = 0, \tag{37}$$

$$\theta'' + \frac{Pr}{2}[1 + x\coth(x)]f\theta' - 2Prx\coth(x)f'\theta + N_\mathrm{b}\sinh(x)\theta' s' + N_\mathrm{t}(\sinh(x))^2(\theta')^2 = 0, \tag{38}$$

$$s'' + \frac{Le}{2}[1 + x\coth(x)]fs' - Lex\coth(x)f's + \frac{N_\mathrm{t}}{N_\mathrm{b}}\sinh(x)\theta'' = 0, \tag{39}$$

with the following boundary conditions

$$f'(\eta, x) = 1,\ \ f(\eta, x) = 0,\ \ \theta(\eta, x) = 1,\ \ s(\eta, x) = 1 \ \text{ at } \ \eta = 0,$$
$$f'(\eta, x) \to 0,\ \ \theta(\eta, x) \to 0,\ \ s(\eta, x) \to 0 \ \text{ as } \ \eta \to \infty. \tag{40}$$

Using differentiation for Eqs. (11)–(13) with respect to $x$ omitting the terms

$$x\left(f'\frac{\partial g'}{\partial x} - f''\frac{\partial g}{\partial x}\right),\ \ x\left(f'\frac{\partial \varphi}{\partial = x} - \theta'\frac{\partial g}{\partial x}\right),\ \ x\left(f'\frac{\partial h}{\partial x} - s'\frac{\partial g}{\partial x}\right),$$

we obtain

$$g''' + \frac{1}{2}[1 + x\coth(x)](fg'' + gf'') + \frac{1}{2}\{\coth(x) + x[1 - \coth^2(x)]\}ff'' - 2x\coth(x)f'g' - \{\coth(x) + x[1 - \coth^2(x)]\}f'^2 - f'g' + f''g - x(g'^2 - g''g) = 0, \tag{41}$$

$$\varphi'' + \frac{Pr}{2}[1 + x\coth(x)](f\varphi' + g\theta') + \frac{Pr}{2}\{\coth(x) + x[1 - \coth^2(x)]\}f\theta' - 2Prx\coth(x)(g'\theta + f'\varphi) - 2Pr\{\coth(x) + x[1 - \coth^2(x)]\}f'\theta + N_\mathrm{b}\sinh(x)(\varphi' s' + \theta' h') + N_\mathrm{b}\cosh(x)\theta' s' + N_\mathrm{t}(\sinh(x))^2\theta'\varphi' + 2N_\mathrm{t}\sinh(x)\cosh(x)(\theta')^2 - f'\varphi + \theta' g - x(g'\varphi - \varphi' g) = 0, \tag{42}$$

$$h'' + \frac{Le}{2}[1 + x\coth(x)](fh' + gs')$$

$$+\frac{Le}{2}\left\{\coth(x)+x\left[1-\coth^2(x)\right]\right\}fs'$$
$$-Lex\coth(x)\left(g's+f'h\right)-Le\left\{\coth(x)+x\left[1-\coth^2(x)\right]\right\}f's$$
$$+\frac{N_t}{N_b}\cosh(x)\theta''+\frac{N_t}{N_b}\sinh(x)\phi''$$
$$+Le\left[\theta'g-f'\varphi-x\left(g'\varphi-\varphi'g\right)\right]=0, \quad (43)$$
$$g'(\eta,x)=1,\ \ g(\eta,x)=0,\ \ \varphi(\eta,x)=1,\ \ h(\eta,x)=1 \ \text{ at } \ \eta=0,$$
$$g'(\eta,x)\to 0,\ \ \varphi(\eta,x)\to 0,\ \ h(\eta,x)\to 0 \ \text{ as } \ \eta\to\infty. \quad (44)$$

The Natcheim–Swigert iteration technique (a shooting method subject to the Runge–Kutta iterative scheme) is used to find the exact numerical solution of Eqs. (37)–(44). The missing conditions $f''(0,x)$, $\theta'(0,x)$, and $\varphi'(0,x)$ are obtained to calculate the local skin friction, Nusselt number and Sherwood number. The numerical and analytical results of local skin friction, Nusselt's number and the Sherwood number are plotted against $x$.

## 4. Results and discussion

The system of Eqs. (10)–(13) involves four parameters namely $N_b$, $N_t$, $Pr$, and $Le$. In nanofluid problems, the effects of $N_b$ and $N_t$ on the temperature and concentration profiles are very important. The effects of these parameters on the Nusselt and Sherwood numbers are also discussed. Since the governing equations are non-similar in nature therefore, both the numerical and analytical results are obtain to gain an appropriate degree of respect for both the solutions.

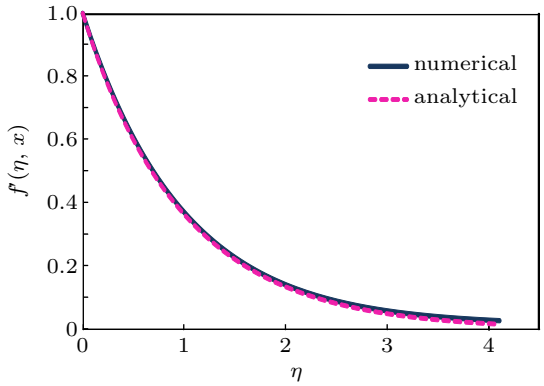



**Fig. 1.** (color online) Comparison of numerical and analytical results of velocity profile for $x = 0.8$.

In Fig. 1, the numerical and analytical results for the velocity profile are plotted for a particular value of $x$. The two results are in an excellent agreement. The velocity profile is plotted in Fig. 2 for different values of $x$. It is found that for a hyperbolic stretching sheet, the momentum boundary layer thickness decays as the distance from the leading edge increases. This is quite reasonable since the momentum boundary layer is proportional to $x/\sqrt{Re_x}$, which in the present case of hyperbolic stretching becomes $\sqrt{x/\sinh(x)}$, which is a decreasing function of $x$. In Fig. 3, we compare numerical and analytical results for skin friction, which are in good agreement up to $x = 2$. It is also observed that the skin friction decreases with an increase in the effect of hyperbolic stretching sheet (increase in $x$). This is in contrast to the linear stretching case where it remains constant along the sheet.

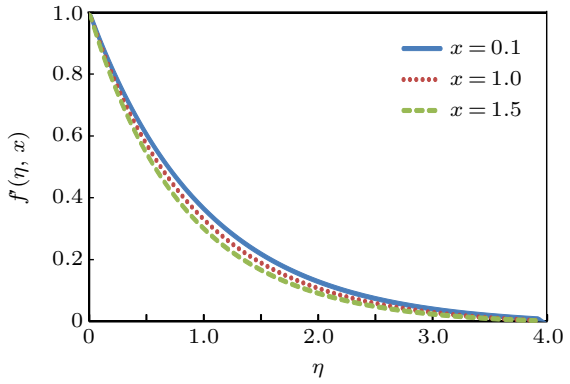



**Fig. 2.** (color online) Velocity profile for different values of $x$.

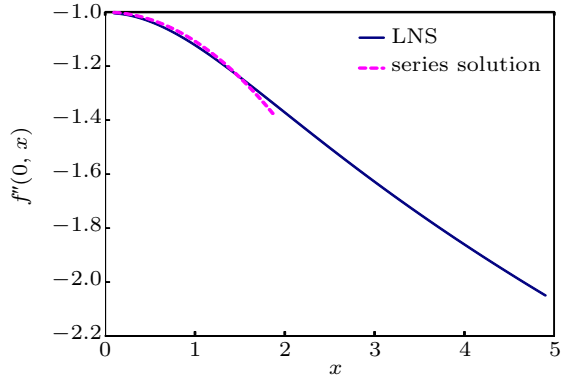



**Fig. 3.** (color online) Comparison of analytical and numerical results of skin friction against $x$. The analytical (series expansion method) result is in good agreement with the numerical (LNS) result for $x$ up to 2.

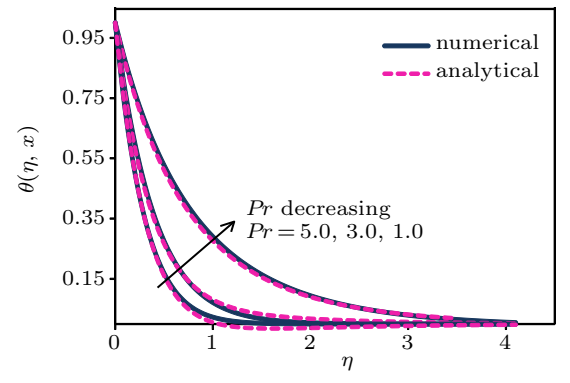



**Fig. 4.** (color online) Comparison of numerical and analytical results of the temperature profile for different $Pr$, where $Le = 2.0$, $N_t = 0.1$, $N_b = 0.1$, and $x = 0.9$.

The numerical and analytical results for the temperature profile have been plotted for different $Pr$ in Fig. 4. The two results are seen to be in good agreement. It is observed from Figs. 4 and 5 that the thickness of the thermal boundary layer

decreases as the Prandtl number increases and the Lewis number decreases. This is because, when the Prandtl numbers increase and the Lewis numbers decrease, the conductivity of the medium decreases, which in turn decreases the thermal boundary layer thickness.

An increase in the temperature of the fluid results in increasing the magnitude of the Brownian motion of particles. This effect can be visualized from Fig. 6 that the curve with a higher temperature corresponds to a higher Brownian motion parameter.

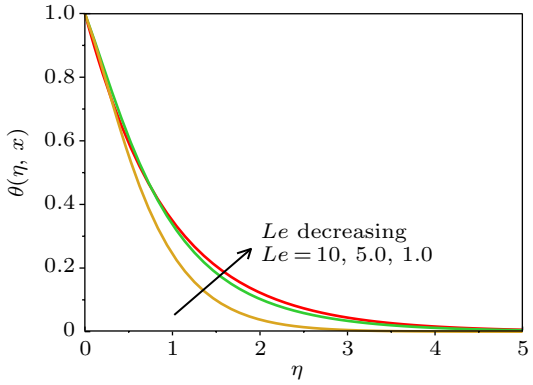



**Fig. 5.** (color online) Temperature profile for different Lewis numbers where $Pr = 1.0$, $N_t = 0.1$, $N_b = 1.0$, and $x = 0.9$.

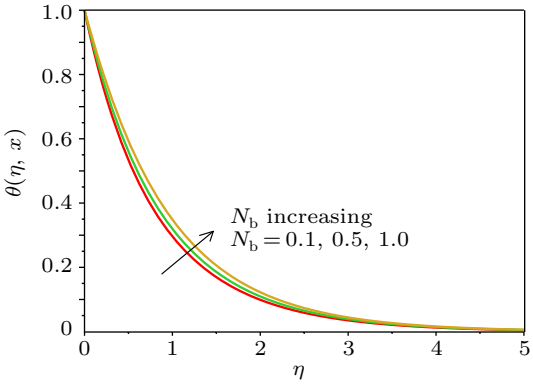



**Fig. 6.** (color online) Temperature profile for different values of Brownian motion where $Pr = 1.0$, $N_t = 0.1$, $Le = 1.0$, and $x = 0.9$.

The effect of $N_t$ on the temperature of the nanofluid is shown in Fig. 7. It is observed that an increase in $N_t$ increases the temperature of the fluid. When $N_t$ increases, the thermal diffusivity of the nanoparticles will accelerate the temperature of the nanofluid. The thermal boundary layer thickness is found to decrease in magnitude as $x$ increases, which is evident from Fig. 8. This consequence can be seen in that the thermal boundary layer is proportional to $\sqrt{x/\sinh(x)Pr^{2/3}}$, which is a decreasing function of $x$.

The numerical and analytical results for different Lewis numbers have been displayed in Fig. 9. Here the agreement between the two solutions is reliable. In fact, the Lewis number is the ratio of conductivity to molecular diffusivity (i.e., Prandtl and schmidth number). Therefore, an increase in $Le$ refers to a decrease in molecular diffusivity and an increase in $Le$ lowers the nanoparticle concentration. This fact can be seen in Fig. 9. An increase in Brownian diffusion parameter $N_b$ refers to an increase in the intermolecular space of nanoparticles. Thus increase in $N_b$ results in lowering the concentration of nanoparticles (see Fig. 10). Figure 11 describes the effect of $N_t$ on nanoparticles concentration. It increases with an increase in $N_t$. In Fig. 12, the nanoparticles concentration profile has been plotted for different values of $x$. For $x = 0$, the results of hyperbolic stretching sheet approach the linear stretching sheet. We observe that with an increase in the effect of the hyperbolic stretching sheet (increase in $x$), the nanoparticle concentration profile decreases.

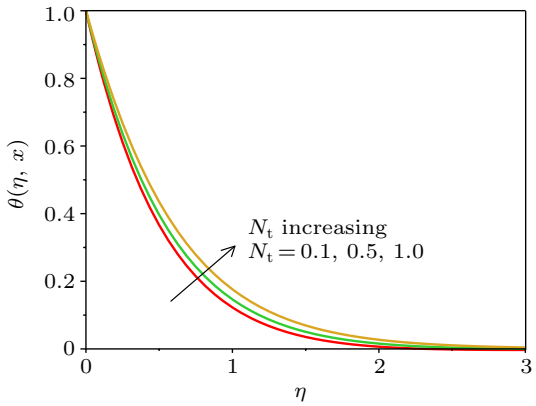



**Fig. 7.** (color online) Temperature profile for different values of $N_t$ where $Pr = 2.0$, $N_b = 0.3$, $Le = 7.0$, and $x = 0.9$.

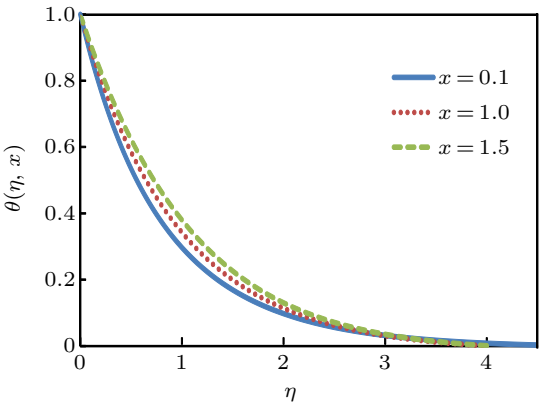



**Fig. 8.** (color online) Temperature profile for different values of $x$ where $Pr = 1.0$, $Le = 1.0$, $N_t = 0.1$, and $N_b = 1.0$.

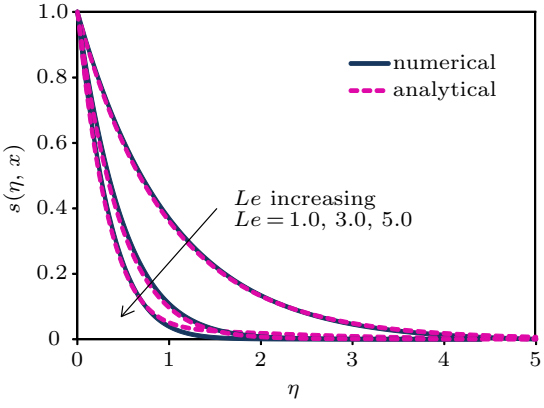



**Fig. 9.** (color online) Comparison of numerical and analytical results for nanoparticles concentration profile for different Lewis numbers where $Pr = 1.0$, $N_t = 0.1$, $N_b = 1.0$, and $x = 0.9$.

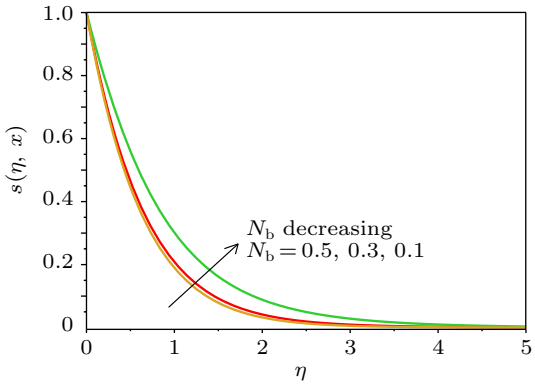



**Fig. 10.** (color online) Nanoparticles concentration profile for different $N_b$ where $Pr = 1.0$, $N_t = 0.1$, $Le = 1.0$, and $x = 0.9$.

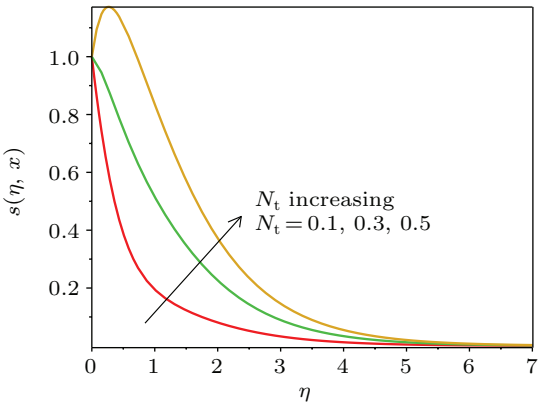



**Fig. 11.** (color online) Nanoparticles concentration profile for different $N_t$ where $Pr = 2.0$, $N_b = 0.1$, $Le = 5.0$, and $x = 0.9$.

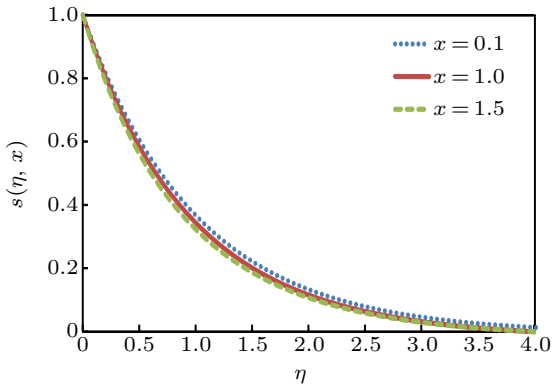



**Fig. 12.** (color online) Nanoparticles concentration profile for different $x$ where $Pr = 1.0$, $Le = 1.0$, $N_t = 0.1$, and $N_b = 1.0$.

The variation of Nusselt number against $x$ has been plotted in Fig. 13 for different values of Brownian diffusion parameter $N_b$. It is seen in Fig. 6 that the temperature of the fluid increases with an increase in $N_b$, which in turn decreases the heat transfer at the surface. This observation is well explained in Fig. 13 that an increase in $N_b$ decreases the Nusselt number. In Fig. 14, the results of Nusselt number for different thermophoresis parameter $N_t$ are sketched against $x$. It is noted that an increase in $N_t$ decreases the Nusselt number. The reason for this behavior of the Nusselt number is obvious from Fig. 7 in which an increase in $N_t$ leads to an increase in temperature, which results in a decreased surface heat transfer.

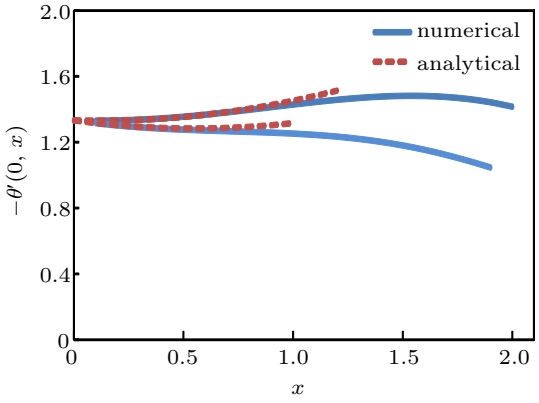



**Fig. 13.** (color online) Nusselt number for different $N_b$ where $Pr = 1.0$, $Le = 1.0$, and $N_t = 0.1$.

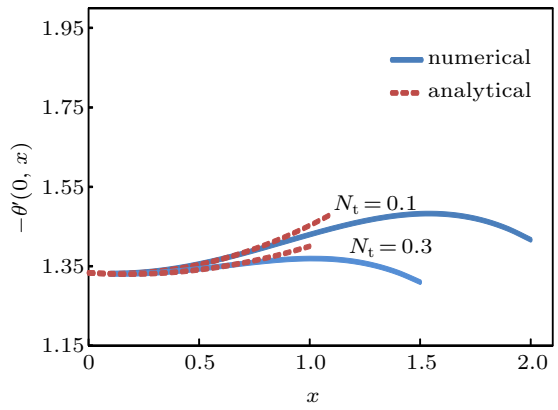



**Fig. 14.** (color online) Nusselt number for different $N_t$ where $Pr = 1.0$, $Le = 1.0$, and $N_b = 0.1$.

It is observed that the Sherwood number decreases by increasing $N_t$ and a decrease in $N_b$ (see Figs. 15 and 16). In Figs. 10 and 11, it is seen that the nanoparticles concentration increases with an increase in $N_t$ and a decrease in $N_b$. This yields a decrease of concentration flux at the surface. In Figs. 13–16, the numerical and analytical results are plotted, which are in an excellent agreement up to $x = 1$.

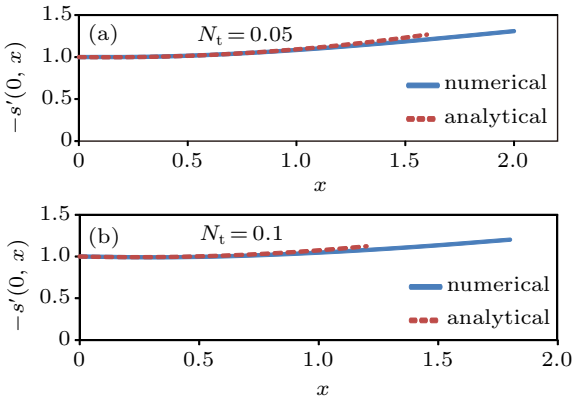



**Fig. 15.** (color online) Sherwood number for different $N_t$ where $Pr = 1.0$, $Le = 1.0$, and $N_b = 1.0$. (a) $N_t = 0.05$, (b) $N_t = 0.1$.

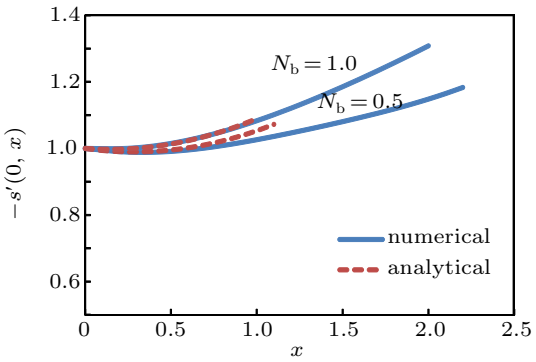



**Fig. 16.** (color online) Sherwood number for different $N_b$ where $Pr = 1.0$, $Le = 1.0$, and $N_t = 0.05$.

## 5. Concluding remarks

The boundary layer flow of nanofluid over a hyperbolic stretching sheet is studied. From the present analysis, we conclude the following results.

1) The leading order solution of this problem represents the flow with heat and mass transfer for traditional viscous fluid over a linearly stretching surface.

2) Effects of Brownian motion and the thermophoretic property of nanofluid are to enhance the temperature of the medium. However, the heat transfer at the surface reduces.

3) The nanoparticle concentration profile decreases as the hyperbolic stretching velocity increases.

4) Thermophoretic property of nanofluid enriches while the Brownian motion of nanoparticles reduces the nanoparticles concentration in the fluid. Opposite effects of these properties of nanofluids are observed for Sherwood number.

## References

[1] Masuda H, Ebata A, Teramae K and Hishinuma N 1993 *Netsu Bussei* **7** 227
[2] Choi S U S 1995 *ASME International Mechanical Engineering Congress and Exposition*, San Francisco, USA, p. 99
[3] Buongiorno J 2006 *ASME J. Heat Tran.* **128** 240
[4] Xiao B Q, Fan J T, Jiang G P and Chen L X 2012 *Acta. Phys. Sin.* **61** 154401 (in Chinese)
[5] Xie H Q and Chen L F 2009 *Acta Phys. Sin.* **58** 2513 (in Chinese)
[6] Xiao B Q 2013 *Chin. Phys. B* **22** 14402
[7] Crane L J 1970 *Z. Angew. Math. Phys.* **21** 645
[8] Kumaran V and Ramanaiah G 1996 *Acta Mech.* **116** 229
[9] Patrick D W and Magyari E 2010 *Acta Mech.* **209** 353
[10] Eerdunbuhe and Temuerchaolu 2012 *Chin. Phys. B* **21** 035201
[11] Magyari E and Keller B 1999 *J. Phys. D: Appl. Phys.* **32** 577
[12] Ahmad A and Asghar S 2012 *Appl. Math. Mech.* **33** 445
[13] Bachok N, Ishak A and Pop I 2010 *Int. J. Therm Sci*. 491663
[14] Khan W A and Pop I 2010 *Int. J. Heat Mass Tran.* **53** 2477
[15] Rana P and Bhargava R 2012 *Commun. Nonlinear Sci. Numer. Simulat.* **17** 212
[16] Nadeem S and Lee C 2012 *Nanoscale Res. Lett.* **7** 94